Hydrological trend analysis in the Yellow River basin using a distributed hydrological model

Zhentao Cong,[1] Dawen Yang,[1] Bing Gao,[1] Hanbo Yang,[1] and Heping Hu[1]

Received 20 January 2008; accepted 3 December 2008; published 24 February 2009.

[1] The hydrological cycle has been highly influenced by climate change and human activities, and it is significant for analyzing the hydrological trends that occurred in past decades in order to understand past changes and to predict future trends. The water crisis of the Yellow River basin has drawn much attention from around the world, especially the drying up of the main river along the lower reaches during the 1990s. By incorporating historical meteorological data and available geographic information related to the conditions of the landscape, a distributed hydrological model has been employed to simulate the natural runoff without consideration of artificial water intake. On the basis of the data observed and the results simulated by the model, the hydrological trends have been analyzed quantitatively for evaluating the impact from climate change and human activity. It is found that the simulated natural runoff follows a similar trend as the precipitation in the entire area being studied during the last half century, and this implies that changes in the natural runoff are mainly controlled by the climate change rather than land use change. Changes in actual evapotranspiration upstream of the Lanzhou gauge are controlled by changes in both precipitation and potential evaporation, while changes of actual evapotranspiration downstream of the Lanzhou gauge are controlled mainly by the changes in precipitation. The difference between the annual observed runoff and the simulated runoff indicates that there is little artificial water consumption upstream of the Lanzhou gauge, but the artificial water consumption becomes larger downstream of the Lanzhou gauge. The artificial water consumption shows a significant increasing trend during the past 50 years and is the main cause of the drying up of the Yellow River. However, in contrast to the common perception that the serious drying up downstream of the Yellow River during the 1990s is caused by the rapid increase of artificial water consumption during the same period, it has been found that the main cause of this aggravation is the drier climate that has existed since the 1990s. The main reason that the drying-up situation became better in the 21st century is because of the enhanced water resources management since 2000.

Citation: Cong, Z., D. Yang, B. Gao, H. Yang, and H. Hu (2009), Hydrological trend analysis in the Yellow River basin using a distributed hydrological model, *Water Resour. Res.*, *45*, W00A13, doi:10.1029/2008WR006852.

1. Introduction

[2] The hydrological cycle traces the largest movement of any substance on Earth [*Chahine*, 1992], and at the same time, has been greatly influenced by climate change and human activities in the past 5–10 decades. Renewable fresh water is the foundation for life in terrestrial and freshwater ecosystems [*Jackson et al.*, 2001]; thus, it is important to analyze the hydrological trends in history for predicting future changes. The components of the regional hydrological cycle include precipitation, evapotranspiration, runoff, and change of water storage, including soil water, groundwater, ice water, snow water, canopy water and reservoir water. Runoff is given more attention for its close relation to the water resources [*McCabe and Wolock*, 1997; *Bronstert et al.*, 2002].

[3] Overall, global land precipitation has increased since the beginning of the 20th century, but the increase is neither spatially nor temporally uniform [*Intergovernmental Panel on Climate Change*, 2007]. Over the last 50 years, there has been a slight decrease in annual precipitation in China [*Zhai et al.*, 1999], including the Yellow River basin [*Yang et al.*, 2004]. As a result, it was found that the runoff was reduced in some major river basins in China, such as the Yangzte River basin [*Yang et al.*, 2005; *Xu et al.*, 2008] and the Yellow River basin [*Fu et al.*, 2004; *Yang et al.*, 2004]. Regarding the evapotranspiration, many observations show that pan or reference evaporation has been steadily decreasing around the world for over the past 50 years [*Peterson et al.*, 1995; *Chattopadhyay and Hulme*, 1997; *Thomas*, 2000; *Liu et al.*, 2004; *Moonen et al.*, 2002; *Roderick and Farquhar*, 2004]. It has been disputed that the decreasing of the pan or reference evaporation predicates the decrease of the actual evaporation [*Peterson et al.*, 1995; *Brutsaert*

[1]State Key Laboratory of Hydro-Science and Engineering and Department of Hydraulic Engineering, Tsinghua University, Beijing, China.

0043-1397/09/2008WR006852$09.00

and Parlange, 1998]. On the basis of the Budyko hypothesis, *Yang et al.* [2006] suggested that a complementary relationship exists in nonhumid areas where the precipitation is the controlling factor of the actual evapotranspiration and that a proportional relationship exists in humid areas where energy is the controlling factor. Quantitative analysis of evapotranspiration is still needed for better understanding of the regional variability of the water balance.

[4] The observation data, including precipitation, runoff, and pan evaporation can be used to analyze the hydrological trend. However, for most rivers we cannot obtain the natural runoff data without knowing the extent of the influence of human activities, and we cannot observe the actual evapotranspiration directly for a catchment. Therefore, the hydrological models are considered as useful tools for analyzing the hydrological trend. Hydrological models have been used widely for water resource assessment, especially for studying the impact of climate change [*Oki et al.*, 2001; *Doll et al.*, 2003]. *Arnell* [1999] used a daily water balance model for investigating the impact of climate change on global water resources. *Nijssen et al.* [2001] used a variable infiltration capacity (VIC) conceptual model [*Liang et al.*, 1994] for global runoff and discharge simulation, while *Middelkoop et al.* [2001] compared a water balance model and a physically based model for water resources assessment in the Rhine basin. The simple biosphere model 2 (SiB2) was used to simulate the potential impacts of land use on surface water fluxes in the Chao Phraya River basin [*Kim et al.*, 2005], and the Community Land Model version 3 (CLM3) was used to analyze the hydroclimatic trends in the Mississippi River basin [*Qian et al.*, 2007]. The geomorphology-based hydrological model (GBHM), a distributed hydrological model, has been successfully used for analyzing the runoff changes in the Chao Phraya River basin [*Yang et al.*, 2001] and the Yangzte River basin [*Xu et al.*, 2008].

[5] The Yellow River, also known as Huanghe in Chinese, is the second-longest river in China with a length of 5464 km. Its basin is also considered the second largest in area, with a drainage area of 752,400 km^2. Over the last 30 years, the Yellow River has become a seasonal river. Drying up of the main river along the lower reaches started in 1972 and has increased rapidly through the years. The most serious drought happened in 1997 when the section close to the sea dried up for more than 226 days and reached a distance of 704 km from the river mouth. Water shortages, especially the drying up of the main river along the lower reaches of the Yellow River, has drawn a lot of attention from all over the world.

[6] Several studies have been commissioned to attempt to explain the changes of the water resources in the Yellow River basin. Historical climate data are generally available and provide a reference for studying the impact of climate change on water resources. Moreover, trend analysis is commonly employed for this purpose [*Fu et al.*, 2004; *Burn and Hag Elnur*, 2002; *Zhang et al.*, 2001]. From these records, it has been noted that the annual precipitation has decreased by 45.3 mm, and the annual mean air temperature has increased by 1.28°C in the Yellow River basin in the last half century. In addition, results of the studies have identified climate change and an increase in artificial water use as the two main factors leading to the drying up of the river [*Yang et al.*, 2004; *Cheng et al.*, 1999]. However, the details are not clear as to the effects of climate change and human activity in the long term. One reason for this information gap is the lack of long-term data on the water intake by the different water sectors such as the irrigation intake, industrial and domestic uses, and water transfer across basins. In addition, irrigation water is not completely consumed in the field through evapotranspiration, as some of it goes back to the river. Therefore, water intake measurements cannot simply be taken as the water consumption. In fact, there was research on the hydrological simulation incorporating anthropogenic processes (mainly the reservoir operation and irrigation) in the hydrological model [*Yang et al.*, 2005]. The result shows that the hydrological model could simulate reasonably the irrigation water consumption in the large irrigation regions which have regular irrigation channel systems. However, the simulated total irrigation water use in the whole basin was smaller than the statistical data. The reason is that the irrigation areas were changed year by year, and the data was missed. Alternatively, the natural runoff can be assessed by distributed hydrological models using historical climate data and actual land use as inputs. The natural runoff is defined as the runoff without artificial water intake and regulation. Together with the observed river discharge data, the direct artificial effect on the river runoff can also be assessed.

[7] In the present study, 50 years of daily meteorological data are used together with the available geographic information related to the land cover and vegetation, and an assessment of the natural river discharge is carried out by applying GBHM for simulating the hydrological cycle over the last 50 years in the Yellow River basin without consideration of the artificial water intake. On the basis of long-term observation and hydrological simulation, the hydrological trends in this basin are analyzed for understanding the influences of climate change and human activity.

2. Methodology

[8] Figure 1 shows the current development of water resources in the Yellow River basin. The main irrigation projects provide 7.13 million ha of irrigation areas, which consume a large amount of surface runoff. The large dams along the main river have a total water storage of 60.7 billion m^3, which has the same magnitude as the annual runoff of the Yellow River. In order to evaluate the effects of artificial water use and climate change, it is necessary to assess the natural runoff without the artificial water intake. The present study employs a distributed model for estimating the natural runoff in this basin over the last 5 decades in which only the natural hydrological processes are included; that is, irrigation and reservoir control are not considered in the hydrological simulation. The distributed model uses a grid system with a 10-km spatial resolution for representing the spatial distribution of climate and soil and a subgrid parameterization scheme for representing the topography and land use. The methodology used for constructing this model includes a subgrid parameterization scheme, a basin subdivision scheme, a physically based hillslope hydrological simulation, and a kinematic wave flow routing method. The land surface conditions considered in the hydrological simulation include the topography, land use, vegetation, and soil. Specifically, the topography and soil are treated as being

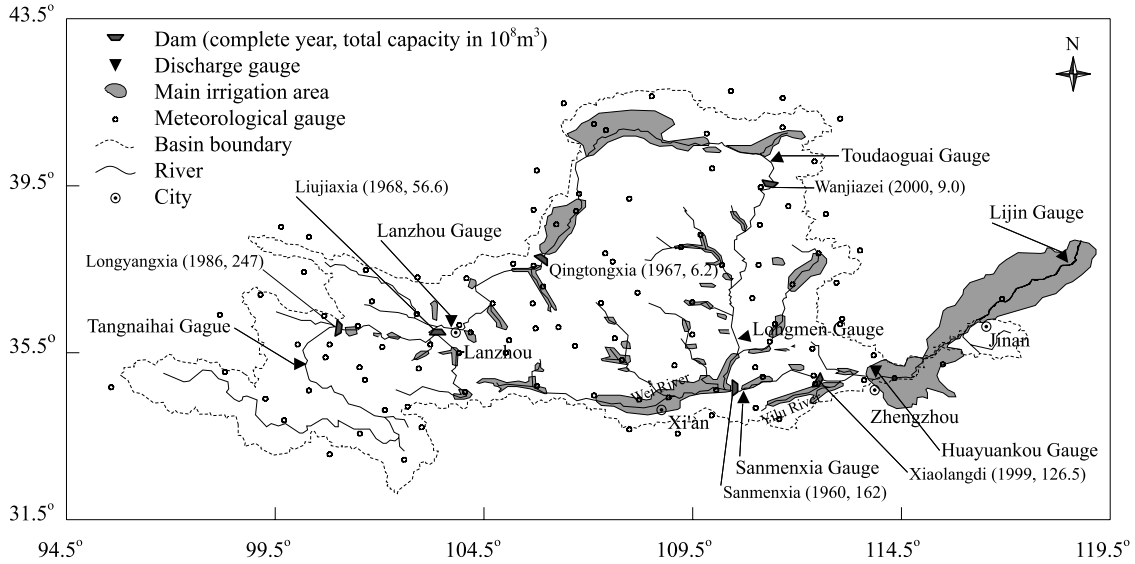

Figure 1. The Yellow River basin (the hydrological simulation area in the study is upstream of the Huayuankou discharge gauge).

constant over time. The model uses the land cover of the 1990s as the base map and considers annual and seasonal changes in vegetation using remotely sensed normalized difference vegetation index (NDVI) data. The atmospheric forcing used in the hydrological simulation is taken from a daily historical climate data set. Since there are significantly fewer drainage areas in the lower reaches (see Figure 1), most of the runoff is generated upstream of the Huayuankou gauge, and therefore, the hydrological simulation covers only this area.

2.1. Data Used in the Study

[9] The geographical information concerning the Yellow River basin used in this research has been obtained from a number of global data sets. The DEM is obtained from the global topography database (http://www2.jpl.nasa.gov/srtm/), which has a 3 arc sec spatial resolution. In this study, the digital elevation model (DEM) is resampled to a 90-m resolution using the Lambert projection coordinate system. Since the model uses a 10-km grid system, the basin base map is regenerated at the same spatial resolution, in which the flow direction of each grid is conceptualized as the main direction. As such, the river basin boundary and the river network are delineated on the basis of this flow direction, and the topographical parameters within a grid are calculated using the 90-m DEM.

[10] Furthermore, data on land cover can be obtained from the U.S. Geological Survey (USGS) Global Land Cover Characteristics Database version 2.0 [*Moody and Strahler*, 1994; *Loveland et al.*, 2000] and has a spatial resolution of 1 km. On the basis of the USGS classification, this land cover map has been regrouped into nine categories, including water bodies, urban areas, bare land, forest, cropland, grassland, wetland, mixtures of bare land and grassland, and ice. The fraction of the area of each land cover type within a 10-km grid is calculated from the 1-km land cover map. For each vegetation type, a monthly leaf area index (LAI) is calculated from the monthly NDVI. A global data set of monthly NDVI with 8-km resolution can be obtained from the DAAC Web site of NASA GSFC (http://daac.gsfc.nasa.gov/) and is available from 1982 onward. The LAI and NDVI before 1982 is used as the average of 1982–1989 data.

[11] The soil type is obtained from the digital soil map of the world and derived soil properties [*Food and Agricultural Organization of the U. N.*, 2003]. It is developed at a 5-min resolution using the FAO-UNESCO soil classification. The effective soil depth is classified into six classes: <10 cm, 10–50 cm, 50–100 cm, 100–150 cm, 150–300 cm, and >300 cm in this data set. A mean value is specified for each class, and the maximum depth is set as 4 m. According to this information, the depth of the unconfined aquifer is somewhat arbitrarily chosen to be 5–10 times the topsoil depth. The soil properties used for the hydrological simulation, including the porosity, the saturated hydraulic conductivity, and the other soil water parameters corresponding to each soil type in this map, are obtained from the Global soil data task [*Data and Information System*, 2000]. The water retention relationship and unsaturated hydraulic conductivity are represented by *van Genuchten*'s [1980] formula, and the parameters are available in this data set. The soil moisture contents at field capacity and wilting point are calculated at matric pressures of −33 and −1500 kPa, respectively. Combining the two soil data sets, the soil type and properties were considered as uniform within a 10-km grid.

[12] The climate data from 1951 to 2000 were obtained from the China Administration of Meteorology. This data set is available at a daily temporal resolution at 108 gauges (see Figure 1). The meteorological inputs include precipitation; maximum, minimum, and mean air temperature; wind speed; relative humidity; and hours of sunshine. The required hydrological girded input is interpolated from the gauge data, while precipitation is interpolated using an angular distance weighing method [*New et al.*, 2000]. In the same way, the wind speed, relative humidity, and hours of sunshine are interpolated into each 10-km grid, whereas the temperatures (maximum, minimum, and mean) are interpolated using an elevation-corrected angular direction

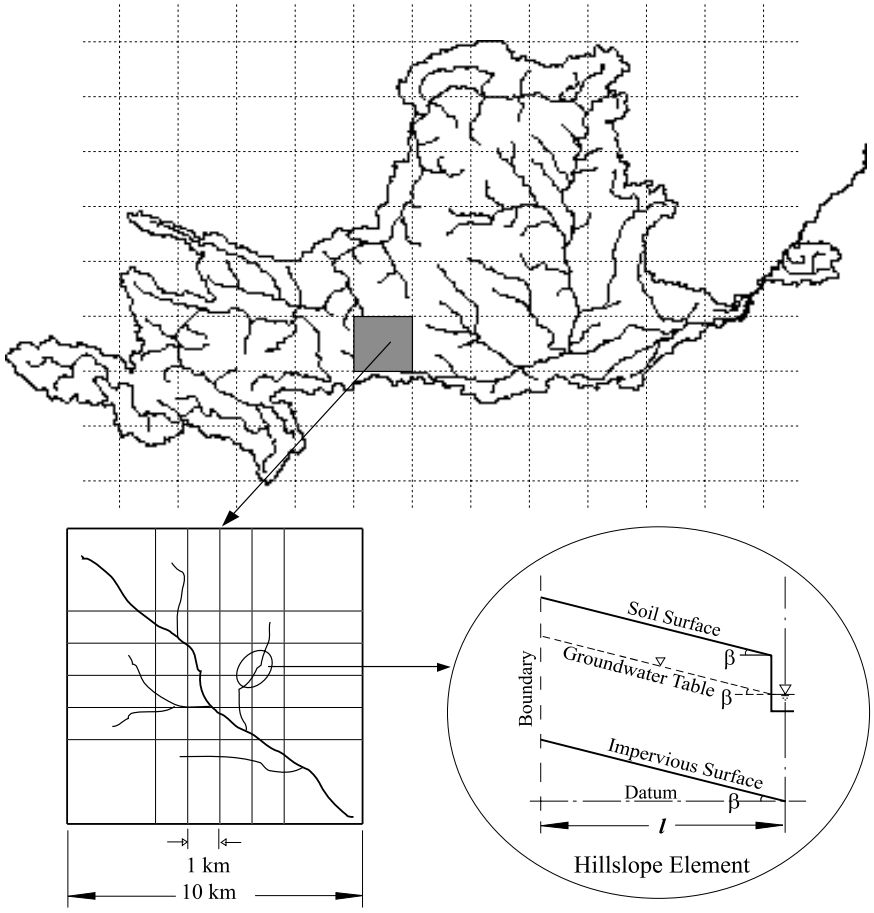

Figure 2. The structure of the hydrological model.

weighing method [*Yang et al.*, 2004] Using the wind speed, relative humidity, sunshine duration, and temperature, the daily potential evaporation is calculated [*Brutsaert*, 1982; *Shuttleworth*, 1993].

[13] The discharge data before 1990 is from the *Hydrological Year Book* published by the Hydrological Bureau of the Ministry of Water Resources of China [*Information Center of Water Resources*, 1950-1990]. The monthly discharge data after 1990 was documented in an annual report by the Hydrological Bureau and is available at the Web site of the Ministry of Water Resources of China (http://www.hydroinfo.gov.cn/zyysq/index.htm). In this study, seven gauges on the main river (see Figure 1) are selected to analyze the change in water resources with respect to river discharges.

2.2. Brief Description of the Distributed Hydrological Model

[14] The present study employs GBHM [*Yang et al.*, 1998, 2000] for estimating the natural runoff in the Yellow River basin, in which only natural hydrological processes are included (there is no consideration of irrigation or reservoir control). The methodology used for constructing this model includes a basin subdivision scheme, a subgrid parameterization scheme, a physically based hydrological simulation on hillslope, and a kinematic wave flow routing method.

[15] For subdividing the Yellow River basin, the Pfafstetter scheme [*Yang and Musiake*, 2003] is applied in the present study. In the present application, a total of 137 subbasins have been identified in the upstream of the Huayuankou gauge. Since the model uses a 10-km grid (see Figure 2), the heterogeneity inside the grid affects the hydrological processes, and therefore, a subgrid parameterization is necessary. The subgrid parameterization used in this research includes representations of the subgrid variabilities in topography and land cover. The topographical parameterization uses the catchment geomorphologic properties, which represents a grid by a number of hillslopes. The hillslopes located in a 10-km grid are grouped according to the land cover types. The hydrological simulation is carried out for each land cover group. The hillslope is a fundamental computational unit for hydrological simulation. A physically based model is used for simulating the hillslope hydrology. The hydrological processes included in this model are snowmelt, canopy interception, evapotranspiration, infiltration, surface flow, subsurface flow, and the exchange between the groundwater and the river [*Yang et al.*, 2002]. The actual evapotranspiration is calculated from the potential evaporation by considering seasonal variation of LAI, root distribution, and soil moisture availability. This is computed individually from the canopy water storage, root zone, and soil surface. Infiltration and water flow in the subsurface in the vertical direction and along the hillslope are described in a quasi-two-dimensional subsurface model.

Table 1. Main Parameters Used in the GBHM

Parameter	Method of Estimation
Vegetation and Land Surface Parameter	
Leaf area index (LAI)	Estimated from MODIS NDVI
Evaporation coefficient	Refer to *Allen et al.* [1998]
Surface retention capacity	Estimated from land use
Surface Manning roughness coefficient	Estimated from land use
Soil Water Parameter	
Saturated volumetric moisture content of topsoil	Obtained from the IGBP-DIS global soil database
Residual volumetric moisture content of topsoil	Obtained from the IGBP-DIS global soil database
Saturated hydraulic conductivity of topsoil	Obtained from the IGBP-DIS global soil database
Parameter for soil water retention curve and hydraulic conductivity in *van Genuchten*'s [1980] equation (unit of matric pressure: cm water)	Obtained from the IGBP-DIS global soil database
River Parameter	
River geometry	Estimated from the measurement data
River Manning roughness coefficient	Refer to *Maidment et al.* [1993]
Other Parameters	
Snowmelt factor in the temperature-based snowmelt equation	Calibrated parameter
Hydraulic conductivity of the groundwater	Calibrated parameter

The vertical water flow in the topsoil is represented by Richards' equation and is solved by an implicit numerical solution scheme. In this scheme, the topsoil is subdivided into a number of layers. Similar to the common subdivision used in many land surface schemes, the topsoil is divided into a near-surface layer of 5 cm, a root zone, and a deep zone. The root zone and deep zone are again derived into sublayers in the present model. The first layer is expected to be saturated during the rainfall period. Therefore, the upper boundary condition is given as constant soil water content for the rainfall cases. During the nonrainfall period, evaporation from the soil surface exists, and the upper boundary condition is given as a constant flux. The soil water distribution along the hillslope is treated as uniform. The surface runoff is from the infiltration excess and saturation excess calculated by solving Richards' equation. The surface runoff flows through the hillslope into the stream via kinematic wave. The groundwater aquifer is treated as an individual storage corresponding to each grid. The exchange between the groundwater and the river water is considered as steady flow and is calculated by Darcy's law [*Yang et al.*, 2002, 2005]. The runoff generated from the grid is the lateral inflow into the river at the same flow interval. Flow routing in the river network is solved using the kinematic wave approach. The parameters used in the hydrological model are listed in Table 1.

2.3. Model Calibration and Validation

[16] As shown in Table 1, there are mainly two parameters, namely, the snowmelt factor in the temperature-based snowmelt equation and the hydraulic conductivity of the groundwater, that need to be calibrated. According to the climate and landscape conditions, three subbasins were selected for the calibration. They were the upstream area of the Tangnaihai gauge, the Wei River basin, and the Yiluo River basin (see Figure 1). The drainage area of the Tangnaihai gauge is about 121,972 km^2. There is little human activity in this region, and the model parameters calibrated during any period can represent the natural hydrological characteristics in the regions of the Tibet plateau. On the basis of the observed daily discharge at the Tangnaihai gauge, a 5-year test run from 1981 to 1985 was carried out for calibration, and another 5-year run from 1986 to 1990 was carried out for validation. For eliminating the impact of human activities downstream of the Tangnaihai gauge, the observed river discharge during the 1950s was used for model calibration in the Wei River basin and in the Yiluo River basin (see Figure 1). The Xianyang gauge (near Xi'an), with a drainage area of 46,827 km^{2}on the Wei River, and the Baimashi gauge (near Zhengzhou) with a drainage area of 11,891 km^2 on the Luo River, were selected. Since there is little snow downstream of the Lanzhou gauge, the snowmelt factor is calibrated on the basis of the hydrograph at the Tangnaihai gauge from March to May. The hydraulic conductivities of the groundwater in the three typical regions were calibrated on the basis of the base flows, which were given as a certain proportion of the saturated hydraulic conductivity of the topsoil.

[17] Figure 3a shows a comparison between the simulated and observed daily discharges at the Tangnaihai gauge for both the calibration and validation periods. On the basis of the daily discharges, the ratio of the absolute error to the mean (R) suggested by the *World Meteorological Organization* [1975] and the Nash coefficient (R^2) introduced by *Nash and Sutcliffe* [1970] are calculated for evaluating the model performance [*Yang et al.*, 2002]. The values of R and R^2 are 19% and 0.88 for the calibration period and 17% and 0.89 for the validation period, respectively. Comparison of the observed and simulated discharges at the Xianyang and Baimashi gauges are shown in Figures 3b and 3c. It can be seen that the simulated daily hydrograph agrees with the

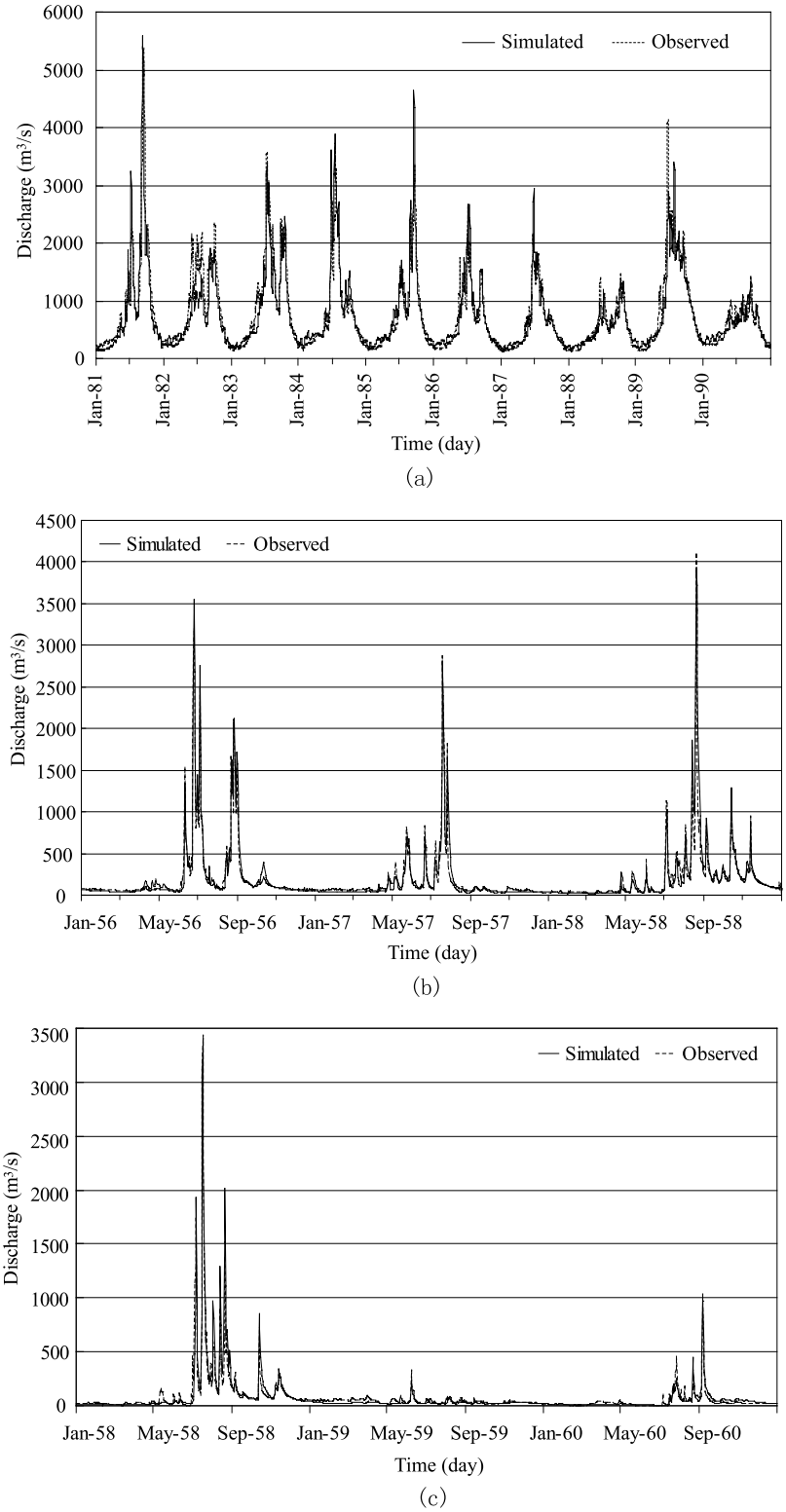

Figure 3. Comparison of simulated and observed daily river discharge (a) at the Tannaihai gauge for the calibration period (1 January 1981 to 31 December 1985) and the validation period (1 January 1986 to 31 December 1990), (b) at the Xianyang gauge from January 1956 to December 1958, and (c) at the Baimaci station from January 1958 to December 1960.

Table 2. Long-Term Average Water Balances From 1951 to 2000[a]

Region	Precipitation (mm/a)			Actual Evaporation (mm/a)			Runoff (mm/a)		
	Annual	Dry	Rain	Annual	Dry	Rain	Annual	Dry	Rain
Upstream of Lanzhou (I)	447	173	274	309	121	189	137	57	79
Lanzhou-Toudaoguai (II)	264	83	180	251	113	139	12.4	6.6	5.6
Toudaoguai-Longmen (III)	420	135	285	382	184	198	42	14.8	23.6
Longmen-Sanmenxia (IV)	548	204	344	468	238	230	84	27	53.7
Sanmenxia-Huayuankou (V)	631	247	384	510	258	253	126	43.3	77
Whole study area	440	159	280	362	168	194	77	30	47

[a]The Yellow River basin is divided into six sections by the discharge gauges, which correspond to the different characteristics of hydrology and water uses (see Figure 1). Annual is for the whole year; the dry season is from November to June; and the wet season (Rain) is from July to October.

observed one, and the result is consistent in both the calibration and validation periods. The water balance errors for three regions were in the range of ±2%, which is an acceptable range for water resources assessment.

[18] In the middle and lower reaches associated with heavy human activities, any observations of groundwater level cannot be used as the initial condition for simulating the natural water resources. For specifying an appropriate initial groundwater level, the present study carries out a 50-year test run from 1951 to 2000 to achieve a stable groundwater level. The groundwater level and soil moisture contents at the end of the test run are then used as the initial conditions for the final simulation of the natural hydrological cycle over the past 50 years for the water resources assessment.

2.4. Trend Analysis

[19] The Mann-Kendall nonparametric test has been recommended as an excellent tool for trend detection [*Maidment et al.*, 1993]. The present study applies this test for detecting the significance of the trends in annual, seasonal, and monthly meteorological and hydrological time series. In order to eliminate the influence of serial correlation on the Mann-Kendall (MK) test, *Kulkarni and von Storch* [1995] proposed to prewhiten a series prior to applying the MK test. For more effectively reducing the effect of serial correlation on the MK test, a modified prewhitening procedure, termed trend-free prewhitening (TFPW), was proposed by *Yue and Wang* [2002] and *Yue et al.* [2002].

[20] In this study, the approach of TFPW has been adopted to eliminate the influence of serial correlation of hydrological and meteorological data series before applying the MK test, and the significance level of the trend test (α) is set at 5%. The slope of the trend is estimated as [*Burn and Hag Elnur*, 2002]

$$\beta = \text{median}\left[\frac{(x_j - x_i)}{(j - i)}\right] \quad (1)$$

for all $i < j$, where β is the trend magnitude. A positive value of β indicates an increasing trend, and a negative value of β indicates a decreasing trend.

3. Hydrological Trends

[21] The trend analyses focus on precipitation, evapotranspiration, and runoff, ignoring the water storage change. The precipitation and potential evaporation changes are the two most important indicators of climate change from the hydrological perspective. The observed runoff incorporates the influence of climate change and human activities. These direct activities include land use change, water intake, and reservoir regulation. In the present study, the runoffs simulated by GBHM from 1951 to 1981 reflect the impact of climate change only since the same land use data have been used in simulation, and the runoffs simulated from 1982 to 2000 reflect the impact of climate and land use changes. Since there is no consideration of water intake, irrigation, and reservoir operation, the simulated runoff is called natural runoff in this paper.

3.1. Long-Term Hydrological Characteristics

3.1.1. Spatial Hydrological Characteristics

[22] The general hydrological characteristics can be found from the annual water balance (see Table 2), which shows high spatial variability in this basin. On the basis of the available data, the annual precipitation ranges from less than 200 mm to more than 700 mm, which increases from north to south and from west to east. The annual actual evapotranspiration ranges from 137 to 589 mm (see Figure 4a). The Wei River basin and the area downstream of the Sanmenxia dam have the highest rate (about 600 mm/a) of evapotranspiration. The annual runoff ranges from 0 to ~345 mm (Figure 4b), which consists of only about 20% of the annual precipitation. The major source areas are located upstream of the Lanzhou gauge, the southern part of the Wei River basin, and downstream of the Sanmenxia dam. It is known that this basin's hydrological conditions are complex, ranging from semihumid to semiarid climates.

[23] From the annual runoff simulated under natural conditions, it can be seen that the major source areas are upstream of the Lanzhou gauge. This region generates about 50% of the basin's total annual runoff, with only 30% of the basin's total area. At the same time, the annual runoff generated from the main tributaries midstream between the Longmen and Sanmenxia gauges shares about 25% of the basin total, the same proportion of the drainage area. The area downstream of the Sanmenxia dam generates about 10% of the basin's total annual runoff with only 6% of the basin's total area. The semiarid region and the loess plateau between the Lanzhou and Longmen gauges generate less runoff compared to their shared drainage areas.

3.1.2. Seasonal Hydrological Characteristics

[24] Considering the seasonal precipitation and water consumption, the year may be divided into a dry season from November to June and a wet season from July to October. Table 2 shows the seasonal characteristics of the

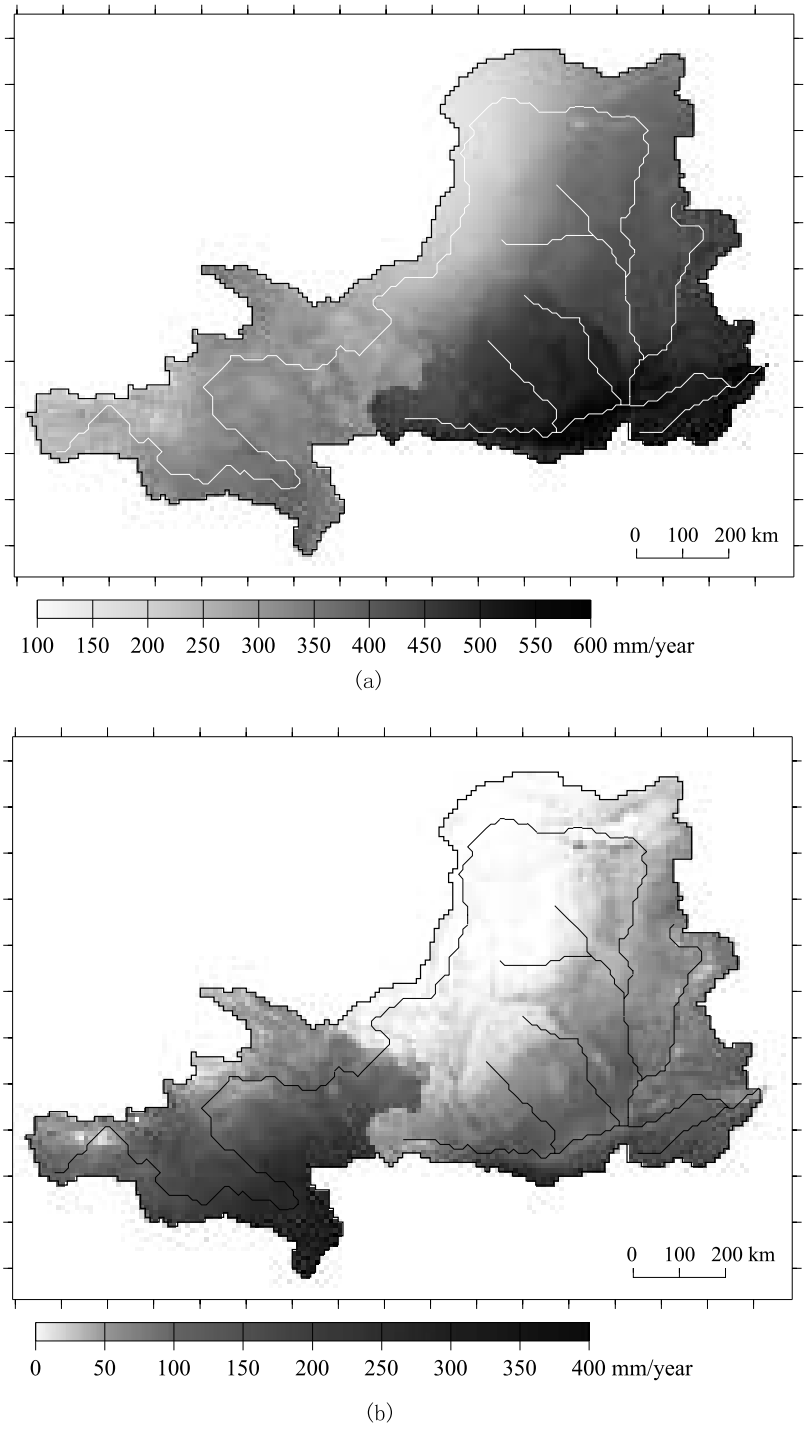

Figure 4. Spatial distributions of the 50-year mean: (a) annual evapotranspiration and (b) annual runoff.

water balance in the study basin. The highly uneven distribution of the seasonal precipitation can be seen from Table 2, in which about 64% of the annual precipitation is concentrated within the wet season from July to October. This seasonally uneven distribution of precipitation is more serious in the semiarid region and the loess plateau (between the Lanzhou and Longmen gauges), where precipitation in the wet season accounts for about 70% of the annual total precipitation. After the land surface hydrological processes, this seasonally uneven distribution of precipitation produces similar uneven seasonal river discharge, and the uneven distribution of the river discharge is amplified in the semiarid region. For the entire simulated area, about 60% of the annual runoff occurs within the wet season from July to October.

3.1.3. Interannual Variability of Runoff

[25] For the annual runoff, the ratio of the maximum value to the minimum value during the last 50 years is 3.0 at the Lanzhou gauge and 4.5 at the Huayuankou gauge. Figure 5 shows the monthly river discharges at the Lanzhou and Huayuankou gauges from 1951 to 2000. The interannual variability of the base flow is much smaller than the peak flow. The variability in the monthly peak discharge is

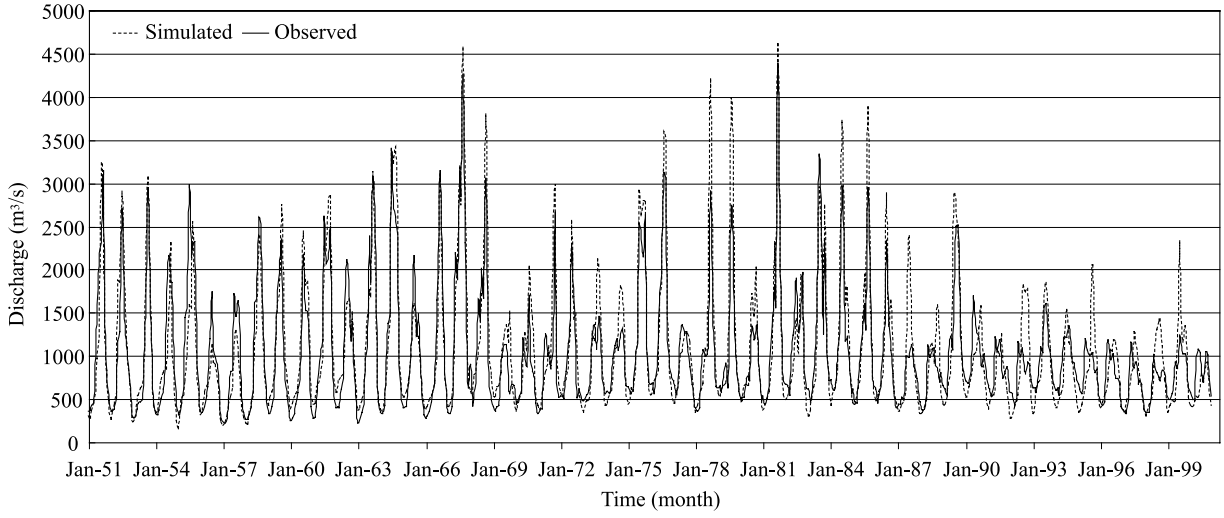

(a) Lanzhou

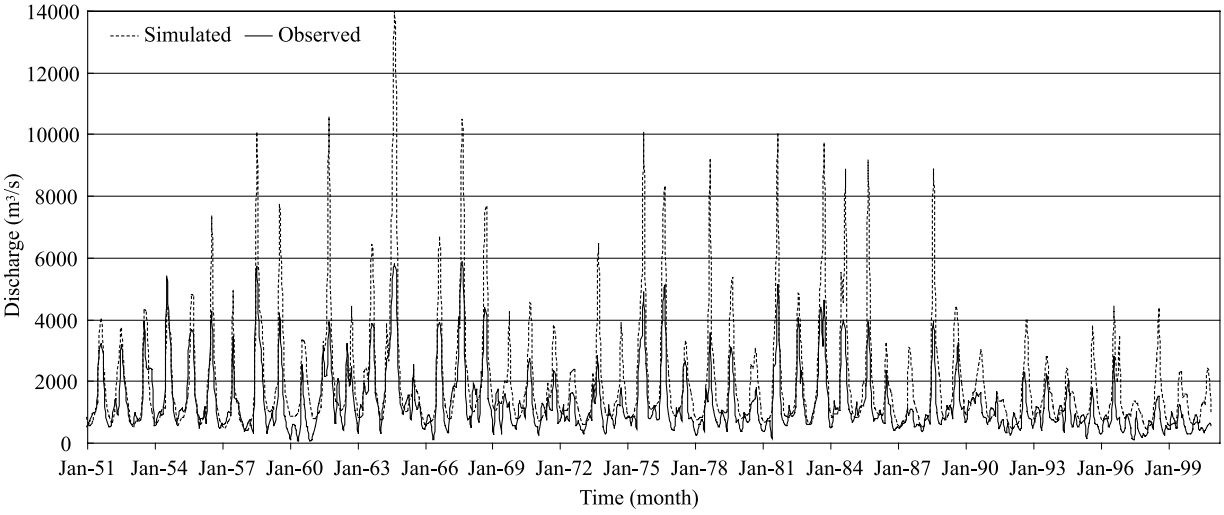

(b) Huayuankou

Figure 5. Monthly river discharge at the Lanzhou and Huayuankou gauges.

about a factor of 5 between a dry year and a wet year at the Lanzhou gauge. This variability is enlarged at the Huayuankou gauge, reaching more than a factor of 10. The high interannual variability of the river discharge determines the likelihood of floods and droughts and makes it difficult to manage the water resources in this basin.

3.2. Hydrological Trends in the Past 50 Years

[26] The hydrological trend and Mann-Kendall test results during the past 50 years are summarized in Table 3. It can be seen that trends of the annual precipitation, pan evaporation, actual evapotranspiration, and natural runoff are not consistent temporally and spatially. During the period of 1951–2000, precipitation shows a slight decreasing trend (nonsignificant) of 4.7 mm/10 a from 1951 to 2000 for the whole study area, and this nonsignificant decreasing trend is found primarily downstream of the Lanzhou gauge; however, the precipitation upstream of the Lanzhou gauge has an increasing trend (nonsignificant). The pan evaporation has a significant decreasing trend of 31.1 mm/10 a for the whole study area, and this decreasing trend is found in both upper and lower parts of the Lanzhou gauge. The actual evaporation has similar trends as precipitation. The simulated natural runoff has significant decreasing trends for both upper and lower reaches of the Lanzhou gauge and the whole study area.

3.2.1. Hydrological Trends Simulated With the Same Land Use From 1951 to 1981

[27] During the period between 1951 and 1981, the precipitation shows a significant increasing trend about 28.3 mm/10 a upstream of the Lanzhou gauge but no significant change downstream of the Lanzhou gauge. The pan evaporation, another indicator of climate change, decreased significantly in the upper reaches of the Lanzhou gauge but increased in the lower reaches of the Lanzhou gauge.

[28] Since the land use from 1951 to 1981 used in the hydrological simulation is adapted from that of the average land use from 1982 to 1989, change trend in the runoff simulated from 1951 to 1981 can be considered to be

Table 3. Hydrological Trend in the Yellow River Basin[a]

Region	Trend (mm/10 a)				Is Kendall Test Accepted?			
	P	ET_p	ET_a	R_{sim}	P	ET_p	ET_a	R_{sim}
			1951–2000					
Upper	7.7	−44.8	14.1	−5.2	N	Y	Y	Y
Lower	−9.9	−21.3	−2.5	−6.3	N	N	N	Y
Whole	−4.7	−31.1	2.4	−5.9	N	Y	N	Y
			1951–1981					
Upper	28.3	−46.3	20.2	10.2	Y	Y	Y	N
Lower	−1.7	56.5	1.0	−0.9	N	N	N	N
Whole	7.2	11.0	6.7	2.4	N	N	Y	N
			1982–2000					
Upper	−27.0	75.6	10.8	−35.7	N	Y	Y	Y
Lower	−33.2	65.7	−6.2	−24.5	Y	Y	N	Y
Whole	−32.4	68.6	−1.2	−28.1	Y	Y	N	Y

[a]Upper, upstream of the Lanzhou gauge; Lower, downstream of the Lanzhou gauge up to the Huayuankou gauge; Whole, the whole study area (up to the Huayuankou gauge); P, annual precipitation; ET_p, annual potential evaporation (here the pan evaporation is used to represent the ET_p); ET_a, annual actual evapotranspiration; and R_{sim}, annual runoff simulated.

influenced mainly by the climate change. Consistent with the precipitation change, the runoff increases for the entire study area and for both the upper and lower reaches of the Lanzhou gauge. It can be concluded that the change trend in river runoff followed the change in precipitation mainly when the land use change can be ignored.

[29] Ignoring the impact of human activity, the actual evapotranspiration is determined by the precipitation and the potential evaporation (here pan evaporation is used for representing the potential evaporation). Comparing the trends of actual evapotranspiration with the trends of the precipitation and pan evaporation, it can be found that change in the actual evapotranspiration in the lower reaches of the Lanzhou gauge is related to both changes of the precipitation and the pan evaporation; however, the trends in actual evapotranspiration in the upper reaches of the Lanzhou gauge is similar to the precipitation trends.

3.2.2. Hydrological Trends Simulated With Actual Land Use From 1982 to 2000

[30] Hydrological simulation by GBHM from 1982 to 2000 is based on the actual vegetation cover so that the hydrological trends can reflect impacts from climate change as well as the change in land use. The precipitation has been reduced during this period both the upstream and downstream of the Lanzhou gauge with the trend of 27.0 mm/10 a (nonsignificant) and 33.3 mm/10 a (significant). At the same time the pan evaporation increased 75.6 mm/10 a (significant) upstream of the Lanzhou gauge and 65.7 mm/10 a (significant) downstream of the Lanzhou gauge. The runoff shows a decreasing trend of 35.7 mm/10 a (significant) and 24.9 mm/10 a (significant) for the upper and lower parts of the Lanzhou gauge, respectively. The actual evapotranspiration increased in the area upstream but decreased in the area downstream of the Lanzhou gauge. The changes of actual evapotranspiration upstream of the Lanzhou gauge are mainly controlled by the potential evaporation change; however, the trend of the actual evapotranspiration downstream of the Lanzhou gauge is mainly controlled by the precipitation change. This implies that the land use change during 1982–2000 does not change the main hydrological pattern responding to the climate.

3.2.3. Trends of the Artificial Water Consumption

[31] The difference between the simulated runoff and the observed runoff can be viewed as the direct human effect on the river runoff, such as water storage, water extraction from the rivers, and water transfer to another basin, with respect to the reduction of river flow. Figure 5 shows the comparison between the simulated and observed discharges at the Lanzhou and Huayuankou gauges. From Figure 5a it can be seen that the difference between the simulated and observed hydrographs is very small during the 1950s and 1960s, but this difference has been enlarged since the 1970s. The reason for this change is the impact of reservoir operation because there is relatively less artificial water consumption in this region. Similarly, it can also be found that the difference between the simulated natural discharge and observed discharge was small in the 1950s for other hydrological stations, and this difference gradually increased (e.g., the Huayuankou gauge in Figure 5b) because of the reservoir regulation and artificial water consumption. The artificial water use is mainly the agricultural irrigation in the Yellow River basin, and the irrigation projects had been constructed since the end of the 1950s. Therefore, we can attribute the difference between simulated and measured annual runoff to the direct human effect on the river runoff, which consists mainly of the artificial water consumption and reservoir storage. Figure 6 shows the difference between the simulated and observed monthly discharges in different decades.

[32] Table 4 summarizes the decadal changes of the hydrological components in different regions since the 1950s. Since there is less artificial water consumption upstream of the Lanzhou gauge, the difference between the simulated and observed runoff is mainly the error of the hydrological simulation. It can be seen that this error is in the range of ±5% except during the 1950s and the period between 2001 and 2005. The reason for relatively larger error may be due to the limited climate data available in the high plateau region during the 1950s and to the reservoir storage increase between 2001 and 2005 because the Yellow River experienced a very dry decade during the 1990s. But downstream of the Lanzhou gauge, the difference between the observed and simulated runoff is much beyond the hydrological simulation error, and the trend can be viewed as the trend of direct artificial effect on the river runoff. The degree of direct artificial effect on the river runoff becomes larger than 70% since the 1970s and larger than 100% since the 1990s. This implies that the artificial water consumption in the region between the Lanzhou gauge and the Huayuankou gauge might be larger than the amount of the runoff generated from the same region since the 1990s. The present situation shows that the runoff generated upstream of the Lanzhou gauge sustains the river flow in the lower reaches of the Yellow River.

[33] Taking the river discharge at the Huayuankou gauge as the naturally available runoff for the whole of the Yellow River basin because of the suspended river along the lower reaches, the direct artificial effect on the river runoff for the whole Yellow River basin can be estimated as the difference between the simulated river discharge at the Huayuankou gauge subtracted from the observed river discharge at the

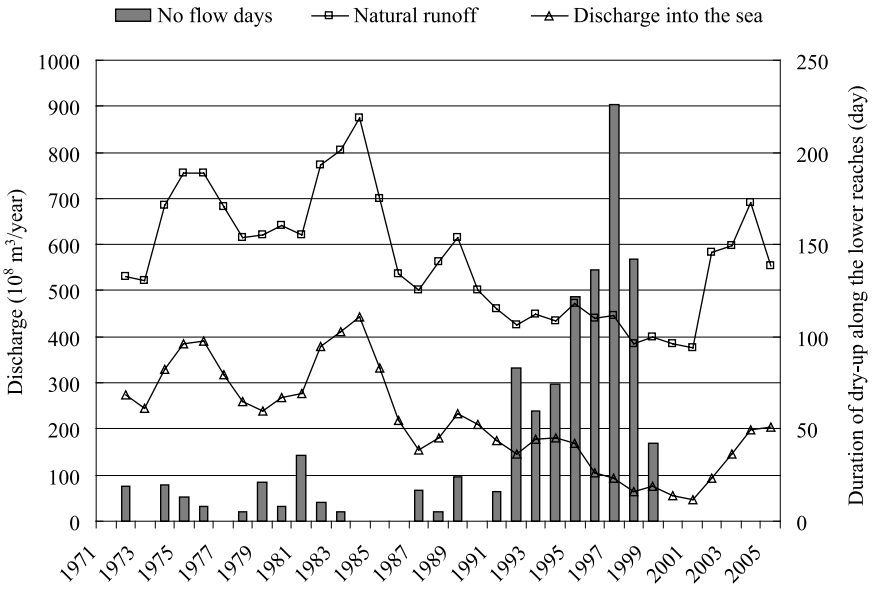

Figure 6. Relationship between the natural runoff, discharge into the sea, and the duration of the dry up (the natural runoff and discharge into the sea are 3-year average values).

Lijin gauge (see the bottom part of Table 4). The degree of direct artificial effect on river runoff continually increased from the 1950s to the present. However, the statistical data of artificial water consumption in the Yellow River basin (see the last row of Table 4) shows that the artificial water consumption does not increase since the 1990s. The river drying up along the lower reaches has been continuously aggravated since the 1970s and was at its worst in the 1990s (see Table 5). It improved during the 21st century. However, the annual discharge into the sea has continuously decreased since the 1970s (see Figure 6), which is closely related to the natural runoff. Therefore, it can be concluded that the main reason for the river dry up is the increase of artificial water consumption; dry climate is the main cause for the desiccation of the lower reaches in the 1990s, and this situation improved during the 21st century mainly as a

Table 4. Hydrological Components of the Different Periods in the Yellow River Basin

Component	1950s	1960s	1970s	1980s	1990s	2001–2005
Upstream of the Lanzhou Gauge						
Precipitation (mm/a)	412.5	459.3	456.0	470.0	434.5	449.6
Actual evaporation (mm/a)	290.2	303.0	308.1	319.1	329.0	326.9
Natural runoff by simulation (mm/a)	121.0	156.3	149.4	149.3	107.2	121.8
Relative error of simulated runoff comparing to the observed one (%)	−7.9	2.3	5.0	0.3	−3.3	9.9
Midstream Between the Lanzhou and Huayuankou Gauges						
Precipitation (mm/a)	451.7	468.8	428.0	436.8	397.6	427.2
Actual evaporation (mm/a)	390.3	395.3	382.5	380.0	372.8	367.6
Natural runoff by simulation (mm/a)	53.8	74.0	48.3	55.9	29.6	53.2
Actual runoff by observation (mm/a)	29	34.1	10.7	16.1	−3.1	−3.5
Direct artificial effect on river runoff[a] (mm/a)	24.8	39.9	37.6	39.8	32.7	56.7
Degree of direct artificial effect on the river runoff[b] (%)	46	54	78	71	110	107
The Whole Simulation Area						
Precipitation (mm/a)	440.2	466.0	436.3	446.6	408.5	443.8
Natural runoff at Huayuankou gauge by simulation ($\times 10^8$ m^3/a)	572.3	763.8	607.1	648.5	407.8	570.9
Direct artificial effect on river runoff[a] ($\times 10^8$ m^3/yr)	134.0	236.4	312.4	355.1	273.4	433.5
Degree of direct artificial effect on the river runoff[b] (%)	23.4	30.9	51.5	54.8	67.1	75.9
Artificial water consumption from statistics ($\times 10^8$ m^3/a)	115.4	162.8	241.7	294.0	285.0	281.1

[a]Direct artificial effect on river runoff is the difference between the simulated and observed river runoff, which includes mainly the artificial water consumption and change of the reservoir water storage.

[b]Degree of direct artificial effect on the river runoff is the ratio of direct artificial effect on river runoff to natural runoff by simulation.

Table 5. Historical Records of River Drying Up Since the 1970s

Year	1971	1972	1973	1974	1975	1976	1977	1978	1979	1980
Days of no flow	0	19	0	20	13	8	0	5	21	8
Maximum distance of on flow (km)	0	310	0	316	278	166	0	104	278	104
Annual discharge into the sea (10^8 m^3)[a]	318.4	222.8	281.5	231.6	478.1	449.1	247.5	259.1	270.0	188.8
Year	1981	1982	1983	1984	1985	1986	1987	1988	1989	1990
Days of no flow	36	10	5	0	0	0	17	5	24	0
Maximum distance of on flow (km)	662	278	104	0	0	0	216	150	277	0
Annual discharge into the sea (10^8 m^3)	346.0	296.9	490.8	446.6	389.0	157.3	108.5	193.8	241.7	264.3
Year	1991	1992	1993	1994	1995	1996	1997	1998	1999	2000
Days of no flow	16	83	60	74	122	136	226	142	42	0
Maximum distance of on flow (km)	131	303	278	380	683	579	704	449	278	0
Annual discharge into the sea (10^8 m^3)	122.5	133.7	185.0	217.0	136.7	155.2	18.6	106.2	68.4	48.6
Year	2001	2002	2003	2004	2005	0	0	0	0	0
Days of no flow	0	0	0	0	0	0	0	0	0	0
Maximum distance of on flow (km)	0	0	0	0	0	0	0	0	0	0
Annual discharge into the sea (10^8 m^3)	46.5	41.9	192.6	198.8	206.8	-	-	-	-	-

[a]Annual discharge into the sea is simply taken as the annual discharge at the Lijin hydrological station.

result of the enhanced water resources management in addition to the climate.

4. Conclusion

[34] Incorporating meteorological data and the available geographic information related to the land surface conditions, a distributed hydrological model (GBHM) has been applied to simulate the hydrological component. On the basis of the data observed and the results simulated, the hydrological trend in the Yellow River basin during the past 50 years was analyzed in the study to explore the changes of water resources and the reason for the drying up of the Yellow River.

[35] Regarding the long-term hydrological characteristics of the basin, the spatial and seasonal distributions of water resources show high variabilities. More than 50% of the basin's total annual runoff is generated upstream of the Lanzhou gauge, which comprises only 30% of the total basin area. About 60% of the annual precipitation is concentrated within the months from July to October. As a result of precipitation through the land surface hydrological processes, the river discharge mediates the seasonal uneven distribution upstream of the Lanzhou gauge, but an enlarged uneven distribution is found downstream of the Lanzhou gauge. The interannual variability of the water resources is also quite large. The monthly peak discharges are different by about a factor of 5 between a dry year and a flood year at the Lanzhou gauge. This variability reaches more than a factor of 10 at the Huayuankou gauge.

[36] Regarding the hydrological trend in this basin, it was found that changes of annual precipitation, pan evaporation, actual evapotranspiration, and natural runoff during the past 50 years were not consistent temporally and spatially. The precipitation had a significant increasing trend upstream of the Lanzhou gauge between 1951 and 1981 but a significant decreasing trend downstream of the Lanzhou gauge between 1982 and 2000. The pan evaporation showed a significant decreasing trend upstream of the Lanzhou gauge during 1951–1981 but showed significant increasing trends in the areas both upstream and downstream of the Lanzhou gauge since 1982. The simulated natural runoff had a similar trend as the precipitation in both upper and lower parts of the Lanzhou gauge for the whole period between 1951 and 2000. Change of the actual evapotranspiration upstream of the Lanzhou gauge was related to changes in both precipitation and potential evaporation. However, the actual evapotranspiration showed similar trends as the precipitation downstream of the Lanzhou gauge, which showed that change of the actual evapotranspiration downstream of the Lanzhou gauge was controlled mainly by the changes in precipitation. Change trend in the natural runoff was mainly controlled by the climate change rather than the land use change in the whole study area.

[37] On the basis of the simulated and observed runoff, it was found that the direct artificial effect on the river runoff continuously increased since the 1950s. And the trend of the drying up along the lower reaches was increased during the past century. This confirmed that the main reason for the river dry up was the increase of artificial water consumption. However, comparing the trends of the natural runoff and artificial water consumption in the 1990s, it is concluded that the aggravation of the drying-up trends during the 1990s is mainly a result of climate change because the 1990s were the driest period experienced since 1951. The discharge into the sea showed a continuous decreasing trend from 1972 to 2005; however, the drying-up situation was improved during the 21st century. This is mainly due to the enhanced management of the water resources in the Yellow River basin in addition to the climate.

[38] **Acknowledgments.** This research was supported by National Natural Science Foundation of China (NSFC) (50509011 and 50721140161). The authors would like to express their appreciation for the grants received to aid in this research.

References

Allen, R., L. Pereira, D. Paes, and M. Smith (1998), Crop evapotranspiration: guidelines for computing crop water requirements, *Irrig. Drain. Pap. 56*, Food and Agric. Organ. of the U. N., Rome.

Arnell, N. W. (1999), Climate change and global water resources, *Global Environ. Change*, *9*, S31–S49, doi:10.1016/S0959-3780(99)00017-5.

Bronstert, A., et al. (2002), Effects of climate and land-use change on storm runoff generation: Present knowledge and modelling capabilities, *Hydrol. Processes*, *16*, 509–529, doi:10.1002/hyp.326.

Brutsaert, W. (1982), *Evaporation Into the Atmosphere*, D. Reidel, Dordrecht, Netherlands.

Brutsaert, W., and M. B. Parlange (1998), Hydrologic cycle explains the evaporation paradox, *Nature*, *396*, 30, doi:10.1038/23845.

Burn, D. H., and M. A. Hag Elnur (2002), Detection of hydrologic trends and variability, *J. Hydrol.*, *255*, 107–122, doi:10.1016/S0022-1694(01) 00514-5.

Chahine, T. M. (1992), The hydrological cycle and its influence on climate, *Nature*, *359*, 373–381, doi:10.1038/359373a0.

Chattopadhyay, N., and M. Hulme (1997), Evaporation and potential evapotranspiration in India under conditions of recent and future climate change, *Agric. For. Meteorol.*, *87*, 55–73, doi:10.1016/S0168-1923 (97)00006-3.

Cheng, X., X. Li, and G. Lu (1999), Characteristics of the river dry-up and variation of water resources in the Yellow River basin (in Chinese), *Adv. Sci. Technol. Water Resour.*, *1*, 34–37.

Data and Information System (2000), Global soil data products (CD-ROM)Int. Geosphere-Biosphere Programme, http://daac.ornl.gov/SOILS/igbp.html, Oak Ridge Natl. Lab. Distrib. Active Arch. Cent., Oak Ridge, Tenn.

Doll, P., F. Kaspar, and B. Lehner (2003), A global hydrological model for deriving water availability indicators: Model tuning and validation, *J. Hydrol.*, *270*, 105–134, doi:10.1016/S0022-1694 (02)00283-4.

Food and Agricultural Organization of the U. N. (2003), Digital soil map of the world and derived soil properties, *Land Water Digital Media Ser. Rev. 1*, Rome.

Fu, G. B., et al. (2004), Hydro-climatic trends of the Yellow River basin for the last 50 years, *Clim. Change*, *65*, 149–178, doi:10.1023/B:CLIM.0000037491.95395.bb.

Information Center of Water Resources (1950–1990), *Hydrological Year Book* (in Chinese), Inf. Cent. of Water Resour., Bur. of Hydrol., Minist. of Water Resour., Beijing.

Intergovernmental Panel on Climate Change (2007), *Climate Change 2007: The Physical Science Basis*, edited by S. Solomon et al., Cambridge Univ. Press, Cambridge, U.K.

Jackson, R. B., et al. (2001), Water in a changing world, *Ecol. Appl.*, *11*, 1027–1045, doi:10.1890/1051-0761 (2001)011[1027:WIACW] 2.0.CO;2.

Kim, W., S. Kanae, Y. Agata, and T. Oki (2005), Simulation of potential impacts of land use/cover changes on surface water fluxes in the Chaophraya river basin, Thailand, *J. Geophys. Res.*, *110*, D08110, doi:10.1029/2004JD004825.

Kulkarni, A., and H. von Storch (1995), Monte Carlo experiments on the effect of serial correlation on the Mann-Kendall test of trend, *Meteorol. Z.*, *4*(2), 82–85.

Liang, X., D. P. Lettenmaier, E. F. Wood, and S. J. Burges (1994), A simple hydrologically based model of land surface water and energy fluxes for general circulation models, *J. Geophys. Res.*, *99*, 14,415–14,428.

Liu, B., M. Xu, M. Henderson, and W. Gong (2004), A spatial analysis of pan evaporation trends in China, 1955–2000, *J. Geophys. Res.*, *109*, D15102, doi:10.1029/2004JD004511.

Loveland, T. R., B. C. Reed, J. F. Brown, D. O. Ohlen, J. Zhu, L. Yang, and J. W. Merchant (2000), Development of a global land cover characteristics database and IGBP DIS cover from 1-km AVHRR data, *Int. J. Remote Sens.*, *21*(6–7), 1303–1330.

Maidment, D. R., et al. (1993), *Handbook of Hydrology*, McGraw-Hill, New York.

McCabe, G. J., and D. M. Wolock (1997), Climate change and the detection of trends in annual runoff, *Clim. Res.*, *8*, 129–134, doi:10.3354/cr008129.

Roderick, M. R., and G. D. Farquhar (2004), Changes in Australian pan evaporation from 1970 to 2002, *Int. J. Climatol.*, *24*, 1077–1090, doi:10.1002/joc.1061.

Middelkoop, H., K. Daamen, D. Gellens, W. Grabs, J. Kwadijk, H. Lang, B. Parmet, B. Schadler, J. Schulla, and K. Wilke (2001), Impact of climate change on hydrological regimes and water resources management in the Rhine basin, *Clim. Change*, *49*, 105–128, doi:10.1023/A:1010784727448.

Moody, A., and A. H. Strahler (1994), Characteristics of composited AVHRR data and problems in their classification, Int, *J. Remote Sens.*, *15*(17), 3473–3491, doi:10.1080/01431169408954341.

Moonen, A. C., et al. (2002), Climate change in Italy indicated by agrometeorological indices over 122 years, *Agric. For. Meteorol.*, *111*, 13–27, doi:10.1016/S0168-1923 (02)00012-6.

Nash, J. E., and J. V. Sutcliffe (1970), River flow forecasting through conceptual models part I-A discussion of principles, *J. Hydrol.*, *10*, 282–290, doi:10.1016/0022-1694 (70)90255-6.

New, M., M. Hulme, and P. Jones (2000), Representing twentieth-century space-time climate variability. Part II: Development of a 1961–96 monthly grids of terrestrial surface climate, *J. Clim.*, *13*, 2217–2238, doi:10.1175/1520-0442 (2000)013<2217:RTCSTC>2.0.CO;2.

Nijssen, B., G. M. O'Donnell, D. P. Lettenmaier, D. Lohmann, and E. F. Wood (2001), Predicting the discharge of global rivers, *J. Clim.*, *14*, 3307–3323, doi:10.1175/1520-0442 (2001)014<3307:PTDOGR>2.0. CO;2.

Oki, T., Y. Agata, S. Kanae, T. Saruhashi, D. Yang, and K. Musiake (2001), Global assessment of current water resources using total runoff integrating pathways, *Hydrol. Sci. J.*, *46*(6), 983–995.

Peterson, T. C., V. S. Golubev, and P. Y. Groisman (1995), Evaporation losing its strength, *Nature*, *377*, 687–688, doi:10.1038/377687b0.

Qian, T. T., A. G. Dai, and K. E. Trenberth (2007), Hydroclimatic trends in the Mississippi River basin from 1948 to 2004, *J. Clim.*, *20*, 4599–4614, doi:10.1175/JCLI4262.1.

Shuttleworth, W. J. (1993), Evaporation, in *Handbook of Hydrology*, edited by D. R. Maidment, pp. 4.1–4.53, McGraw-Hill, New York.

Thomas, A. (2000), Spatial and temporal characteristics of potential evapotranspiration trends over China, *Int. J. Climatol.*, *20*, 381–396, doi:10.1002/ (SICI)1097-0088 (20000330)20:4<381::AID-JOC477>3.0. CO;2-K.

van Genuchten, M. (1980), A closed-form equation for predicting the hydraulic conductivity of unsaturated soil, *J. Soil Sci. Soc. Am.*, *32*, 329–334.

World Meteorological Organization (1975), Intercomparison of conceptual models used in operational hydrological forecasting, *WMO Oper. Hydrol. Rep. 7*, Geneva, Switzerland.

Xu, J., D. Yang, Z. Lei, J. Chen, and W. Yang (2008), Spatial and temporal variation of runoff in the Yangtze River basin during the past 40 years, *Quat. Int.*, *186*(1), 32–42, doi:10.1016/j.quaint.2007.10.014.

Yang, D., and K. Musiake (2003), A continental scale hydrological model using distributed approach and its application to Asia, *Hydrol. Processes*, *17*, 2855–2869, doi:10.1002/hyp.1438.

Yang, D., S. Herath, and K. Musiake (1998), Development of a geomorphology-based hydrological model for large catchments, *Annu. J. Hydraul. Eng.*, *42*, 169–174.

Yang, D., S. Herath, and K. Musiake (2000), Comparison of different distributed hydrological models for characterization of catchment spatial variability, *Hydrol. Processes*, *14*, 403–416, doi:10.1002/ (SICI)1099-1085(20000228)14:3<403::AID-HYP945>3.0.CO;2-3.

Yang, D., S. Kanae, T. Oki, and K. Musiake (2001), Expanding the distributed hydrological modelling to continental scale, *IAHS Publ.*, *270*, 125–134.

Yang, D., S. Herath, and K. Musiake (2002), Hillslope-based hydrological model using catchment area and width functions, *Hydrol. Sci. J.*, *47*(1), 49–65.

Yang, D., C. Li, H. Hu, Z. Lei, S. Yang, T. Kusuda, T. Koike, and K. Musiake (2004), Analysis of water resources variability in the Yellow River of China during the last half century using historical data, *Water Resour. Res.*, *40*, W06502, doi:10.1029/2003WR002763.

Yang, D., F. Sun, Z. Liu, Z. Cong, and Z. Lei (2006), Interpreting the complementary relationship in non-humid environments based on the Budyko and Penman hypotheses, *Geophys. Res. Lett.*, *33*, L18402, doi:10.1029/2006GL027657.

Yang, S. L., et al. (2005), Trends in annual discharge from the Yangtze River to the sea (1865–2004), *Hydrol. Sci. J.*, *50*(5), 825–836, doi:10.1623/hysj.2005.50.5.825.

Yue, S., and C. Y. Wang (2002), Applicability of prewhitening to eliminate the influence of serial correlation on the Mann-Kendall test, *Water Resour. Res.*, *38*(6), 1068, doi:10.1029/2001WR000861.

Yue, S., P. Pilon, B. Phinney, and G. Cavadias (2002), The influence of autocorrelation on the ability to detect trend in hydrological series, *Hydrol. Processes*, *16*, 1807–1829, doi:10.1002/hyp.1095.

Zhai, P. M., A. Sun, F. M. Ren, X. Liu, B. Gao, and Q. Zhang (1999), Changes of climate extremes in China, *Clim. Change*, *42*, 203–218, doi:10.1023/A:1005428602279.

Zhang, X., K. D. Harvey, W. D. Hogg, and T. R. Yuzyk (2001), Trends in Canadian streamflow, *Water Resour. Res.*, *37*, 987–998, doi:10.1029/2000WR900357.

Z. Cong, B. Gao, H. Hu, D. Yang, and H. Yang, Department of Hydraulic Engineering, Tsinghua University, Beijing, 100084, China. (yangdw@tsinghua.edu.cn)